PHYSICAL REVIEW E **73**, 011204 (2006)

Concentration-dependent diffusivity and anomalous diffusion: A magnetic resonance imaging study of water ingress in porous zeolite

Eduardo N. de Azevedo, Paulo L. de Sousa, Ricardo E. de Souza, and M. Engelsberg
Departamento de Física, Universidade Federal de Pernambuco, Cidade Universitária, 50.670-901, Recife, Pernambuco, Brazil

Mirla de N. do N. Miranda and Maria Aparecida Silva
Faculdade de Engenharia Química, Universidade Estadual de Campinas. (UNICAMP), 130831-970, Campinas, São Paulo, Brazil

(Received 14 July 2005; published 31 January 2006)

Magnetic resonance imaging is employed to study water ingress in fine zeolite powders compacted by high pressure. The experimental conditions are chosen such that the applicability of Boltzmann's transformation of the one-dimensional diffusion equation is approximately satisfied. The measured moisture profiles indicate subdiffusive behavior with a spatiotemporal scaling variable $\eta = x/t^{\gamma/2}$ $(0 < \gamma < 1)$. A time-fractional diffusion equation model of anomalous diffusion is adopted to analyze the data, and an expression that yields the moisture dependence of the generalized diffusivity is derived and applied to our measured profiles. In spite of the differences between systems exhibiting different values of γ a striking similarity in the moisture dependence of the diffusivity is apparent. This suggests that the model addresses the underlying physical processes involved in water transport.

DOI: 10.1103/PhysRevE.73.011204 PACS number(s): 82.56.Lz, 76.60.Pc

I. INTRODUCTION

The type of anomalous diffusion known as subdiffusion has been observed in a variety of structures [1–4]. Assuming a constant generalized diffusivity D_γ $(\mathrm{cm}^2/\mathrm{sec}^\gamma)$ subdiffusion can be characterized, in one dimension, by a mean square displacement of form [5]

$$\langle (\Delta x)^2 \rangle = \frac{2D_\gamma t^\gamma}{\Gamma(1+\gamma)}, \tag{1}$$

where $0 < \gamma < 1$ and $\Gamma(z)$ denotes Euler's gamma function.

When a macroscopic concentration gradient exists in real systems obeying normal $(\gamma = 1)$ diffusion, the Fickian diffusivity cannot be expected, in general, to be a constant but will actually vary with the local concentration of the diffusing species. A similar behavior can be expected when subdiffusive transport prevails. Magnetic resonance imaging (MRI) is especially useful to monitor water transport in solids and to ascertain whether the transport mechanism is actually diffusive. If this is the case, it is further possible, in general, to determine the dependence of the diffusivity upon the concentration of the diffuser. In a classic example of such an application of MRI, the spatiotemporal dependence of the ingress of water in Nylon 6.6 was studied by Blackband and Mansfield [6]. It was found that, for a considerable range of variables, the process obeys normal diffusion $(\gamma = 1)$ but with a diffusivity which increases exponentially with increasing water concentration.

The basic approach [6,7] for implementing a MRI test of this type is to approximate the conditions for the validity of Boltzmann's transformation of the one-dimensional diffusion equation [7]. Denoting by $W(x,t)$ the local water concentration in a representative volume element (volume of water/total volume of element), the normal diffusion equation $(\gamma = 1)$ can be written in the form

$$\frac{\partial W(x,t)}{\partial t} = \frac{\partial}{\partial x}\left(D_1 \frac{\partial W(x,t)}{\partial x} \right), \tag{2}$$

where D_1 is the normal Fickian diffusivity $D_1(W)$, assumed to be a function only of the concentration of the diffusing species. It is related to the self- diffusion coefficient, measured in the absence of macroscopic concentration gradients [6], through Darken's relationship, which involves the derivative of the chemical potential with respect to W.

If a semi-infinite $(x \geq 0)$ solid is maintained in contact with a water reservoir placed at $x < 0$, such that $W(0,t) = W_0$ for $t > 0$ and $W(x,0) = 0$, Eq. (2) can be considerably simplified. This can be achieved by first introducing a new variable $\eta = x/t^{1/2}$ in Eq. (2), which yields

$$-\frac{1}{2}\eta \frac{dW}{d\eta} = \frac{d}{d\eta}\left(D_1(W) \frac{dW}{d\eta} \right). \tag{3}$$

Furthermore, for the proposed configuration, the boundary conditions can be expressed in terms of the single variable η (for $t > 0$):

$$W(\eta = 0) = W_0 \quad \text{and} \quad W(\eta \to \infty) = 0. \tag{4}$$

Since not only Eq. (3) but also the boundary conditions of Eq. (4) are functions of η alone, the same should hold for $W(\eta)$. Thus, a universal curve would be obtained when the concentration profiles W/W_0, for all values of x and t, are plotted as a function of the scaling variable $\eta = x/t^{0.5}$. It is worth noticing that the assumption of a concentration-dependent diffusivity is essential to obtain a scaling variable that yields a universal curve. For other assumptions, such as a diffusivity $D(x)$ depending only upon the spatial coordinate, for example, such universal behavior is not warranted. Equations (3) and (4) also permit us to determine $D_1(W)$, which can be seen, by a simple integration of Eq. (3), to be given by [7]

$$D_1(W) = -(1/2)\left(\frac{d\eta}{dW}\right)\int_0^W \eta(W')dW'. \quad (5)$$

In this paper we report the results of MRI measurements of water ingress in a porous system consisting of fine particles of zeolite compacted by high pressure where, for a certain range of the variables, the conditions for the validity of Boltzmann's test could be approximately met. Earlier MRI studies of water transport were performed on loosely packed zeolite powders using different boundary conditions [8,9].

Our results reveal subdiffusive behavior with a scaling variable of form $x/t^{\gamma/2}$ $(0<\gamma<1)$, which leads to a universal behavior over a considerable range of data. We next consider the concentration dependence $D_\gamma(W)$ of the anomalous diffusivity and derive an extension of Eq. (5) valid for $\gamma<1$. To that end we employ a generalization of the one-dimensional diffusion equation based upon the concept of time-fractional derivatives [10] to model subdiffusive behavior. The results obtained for $D_\gamma(W)$ by applying the time-fractional approach model to experimental data with various values of γ are compared.

II. ANOMALOUS DIFFUSION

Several generalizations of Eq. (2) have been proposed as models of anomalous diffusion. Especially interesting is the study of the time-fractional diffusion equation [11–17], closely related to fractal time Brownian motion. One way of generalizing Eq. (2) is by writing [12,16] for $0<\gamma<1$

$$\frac{\partial^\gamma W(x,t)}{\partial t^\gamma} - \frac{t^{-\gamma}}{\Gamma(1-\gamma)}W(x,0) = \frac{\partial}{\partial x}\left(D_\gamma \frac{\partial W(x,t)}{\partial x}\right), \quad (6)$$

where D_γ is allowed to be a function of W. Here $\partial^\beta/\partial t^\beta$ denotes a Riemann-Liouville fractional derivative operator defined by

$$\frac{\partial^\beta W(x,t)}{\partial t^\beta} = \frac{1}{\Gamma(1-\beta)}\frac{\partial}{\partial t}\int_0^t \frac{W(x,t')}{(t-t')^\beta}dt', \quad 0 \leqslant \beta < 1, \quad (7)$$

or, for negative β, a fractional integral operator defined by

$$\frac{\partial^\beta W(x,t)}{\partial t^\beta} = \frac{1}{\Gamma(-\beta)}\int_0^t \frac{W(x,t')}{(t-t')^{1+\beta}}dt', \quad \beta<0. \quad (8)$$

We first consider the case of boundary conditions of the form $W_\delta(x,0)=\delta(x)$ and $W_\delta(x,t)\to 0$ for $x\to\pm\infty$. An integration of both sides of Eq. (6) over all values of x, together with the result $\partial^\gamma 1/\partial t^\gamma = t^{-\gamma}/\Gamma(1-\gamma)$ obtained from Eq. (7) for $0<\gamma<1$, yields the normalization condition $\int_{-\infty}^{\infty} W_\delta(x,t)dx=1$. In a somewhat similar manner, multiplication of both sides of Eq. (6) by x^2 and integration over all values of x readily yields, for constant D_γ, the expression for the mean square displacement of Eq. (1).

For the above δ function boundary conditions and for constant D_γ the solution $W_\delta(x,t)$ of the integro-differential equation resulting from Eq. (6) is given by a one-sided stable Lévy density [13] and can also be expressed by the following power series [13,16]:

$$W_\delta(x,t) = \frac{1}{2\pi\sqrt{D_\gamma}t^{\gamma/2}}\sum_{m=0}^{\infty}\frac{(-\zeta)^{m-1}}{(m-1)!}\Gamma(m\gamma/2)\sin(m\pi\gamma/2), \quad (9)$$

where $\zeta = |x|/\sqrt{D_\gamma}t^{\gamma/2}$. Moreover, $W_\delta(x,t)$ can also be shown to be connected to the Gaussian solution, corresponding to $\gamma=1$, by an integral transformation [12].

We can take advantage of $W_\delta(x,t)$ given by Eq. (9) to find the solution for the specific boundary conditions required for Boltzmann's transformation provided a constant diffusivity is assumed. Defining $\Phi(x,t)=W(x,t)/W_0$ in Eq. (6) we notice that the boundary condition $W_\delta(x,0)=\delta(x)$ which leads to the result that $W_\delta(x,t)$ must now be substituted by $\Phi(x,0)=2\int_x^\infty \delta(x')dx'$ for $x\geqslant 0$. Hence, by integrating both sides of Eq. (6) with the δ function boundary condition, the solution can be found to be $1/2\,\Phi(x,t)=\int_x^\infty W_\delta(x',t)dx'$ $(x\geqslant 0)$, which can also be written as $\Phi(x,t)=1-2\int_0^x W_\delta(x',t)dx'$. Moreover, using the series expansion in Eq. (9) we obtain

$$\Phi(\zeta) = 1 - \left(\frac{1}{\pi}\right)\sum_{m=1}^{\infty}\frac{(-1)^{m-1}\zeta^m}{m!}\Gamma(m\gamma/2)\sin(m\pi\gamma/2). \quad (10)$$

The solution for $x\geqslant 0$ can be seen to be only a function of $\xi = x/\sqrt{D_\gamma}t^{\gamma/2}$ $(t>0)$ which reduces to the known result $\Phi(\zeta)=1-(2/\sqrt{\pi})\int_0^{\zeta/2}\exp(-t^2)dt = 1-\mathrm{erf}(\zeta/2)$ when $\gamma=1$.

Finally, we consider the case where the diffusivity is not constant but rather a function of the concentration of diffusers [17]. We seek a generalization of Eq. (5) valid for $0<\gamma<1$. The boundary conditions for Boltzmann's transformation are satisfied if, for $x>0$, the term containing $W(x,0)$ in Eq. (6) is dropped. One can then write, for $\Phi(x,t)=W(x,t)/W_0$,

$$\frac{1}{\Gamma(1-\gamma)}\frac{\partial}{\partial t}\int_0^t \frac{\Phi(x,t')}{(t-t')^\gamma}dt' = \frac{\partial}{\partial x}\left(D_\gamma(\Phi)\frac{\partial\Phi(x,t)}{\partial x}\right). \quad (11)$$

Changing variables to $u=t'/t$ and $\eta = x/t^{\gamma/2}$ in Eq. (11) and performing the time derivative on the left hand side of Eq. (11), assuming Φ to be a function of η only, yields the following integro-differential equation:

$$\frac{1}{\Gamma(1-\gamma)}\int_0^1 \left((1-\gamma)\Phi(\eta/u^{\gamma/2}) - (\gamma/2)\,\eta\frac{\partial\Phi(\eta/u^{\gamma/2})}{\partial\eta}\right) \times \frac{du}{(1-u)^\gamma} = \frac{\partial}{\partial\eta}\left(D_\gamma(\Phi)\frac{\partial\Phi}{\partial\eta}\right). \quad (12)$$

As expected, only the scaling variable $\eta = x/t^{\gamma/2}$ appears in Eq. (12) as well as in the boundary conditions.

It is more convenient to further change to a new variable $\lambda = \eta/u^{\gamma/2}$ in Eq. (12) and integrate both sides with respect to η, yielding

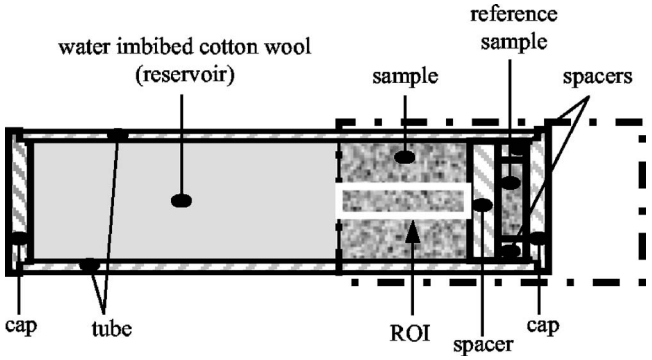

FIG. 1. Longitudinal section of the sample holder. The region of the sample limited by a white rectangle is the region of interest (ROI) for profile calculations. The dot-dashed rectangle indicates the most homogeneous region of the receiver coil.

$$D_\gamma = \frac{d\eta}{d\Phi}\frac{1}{\Gamma(1-\gamma)}\int_\infty^\eta d\eta' \int_{\eta'}^\infty \left((2/\gamma)(1-\gamma)\frac{\Phi(\lambda)}{\lambda} - \frac{d\Phi(\lambda)}{d\lambda}\right)\frac{(\eta'/\lambda)^{2/\gamma}d\lambda}{[1-(\eta'/\lambda)^{2/\gamma}]^\gamma}. \quad (13)$$

Equation (13) is the sought generalization of Eq. (5) for $0 < \gamma < 1$ based upon a time-fractional derivative approach to anomalous diffusion. It permits us to determine $D_\gamma(\eta)$ and $D_\gamma(\Phi)$ from measured values of $\Phi(\eta)$.

III. EXPERIMENTAL DETAILS

The measurements were made at 85 MHz using a Varian Unity Inova spectrometer which includes a 2 T, 30 cm bore superconducting magnet. Figure 1 shows a schematic drawing of the sample holder, which was designed to maximize the filling factor of a specific receiver coil. All experiments were carried out with horizontal fluid uptake at 25 °C and gravitational effects on fluid transport were neglected.

The samples used in the experiments were cylindrical rods 5 cm in diameter and with length varying between 5.0 and 6.0 cm. They were prepared by compressing somewhat moist zeolite NaY (Aldrich, lot 13322PU, average diameter 6 μm) fine powder into a steel mold under an applied pressure of approximately 15 MPa and dried to remove all water prior to MRI measurements. This water removal procedure in materials like zeolites containing intraparticle pores of nanometric diameter is especially sensitive to a form of damage called steaming. Steaming occurs when internal vapor pressure causes damage to the structure of the sample. Specifically in the case of zeolites a vaporizing and recondensing of water within the sample causes recrystallization. To avoid steaming, it was found to be necessary [18] to slowly remove the majority of the water at less than 100 °C and then increase the temperature in a stepwise manner.

In order to implement a reservoir with constant water content, while avoiding direct immersion in water which could cause a partial disintegration of the fine particle zeolite rod, the following arrangement was employed. We assembled a cylindrical tube filled with water-saturated cotton wool and placed it in contact with one of the flat surfaces of the zeolite rod with all other surfaces covered by cellophane. The reservoir contains considerably more water than the amount that ingresses into the samples during the experimental observation and maintains the water content at the interface at the capillary saturation value.

Since some measurements could take several hours, appreciable fluctuations in the receiver gain cannot be ruled out. We therefore introduced a sealed reference sample which permitted us to make corrections of any changes in electronic gain of the receiver system of the spectrometer that could have taken place during the experiments. In order to minimize the NMR signal from the water reservoir, the sample holder was positioned shifted from the receiver coil center, as shown in Fig. 1. This permits the receiver gain to be increased, allowing a wider dynamic range and more accurate measurements of the water uptake. All the longitudinal slices have 2×2 mm^2 in-plane pixel resolution and 1 mm in thickness.

Figure 2 shows NMR images of longitudinal slices taken at 31 and 182 min after the beginning of water uptake. The dark belly-shaped region on the left side of the images is an artifact due to spatial inhomogeneity of the rf field.

From the NMR images we next calculate signal profiles along the symmetry axis of the cylinder. In order to approximate the conditions for the validity of Boltzmann's transformation we consider, for profile calculations, an average signal taken over all the voxels in the ROI (Figs. 1 and 2), chosen to be a small concentric cylinder of 1.5 cm in diameter. Signals from this ROI, for not too long times, should be relatively little dependent upon boundary effects.

In order to convert signal profiles into water content profiles $W(x,t)$ a calibration curve, based upon separate spin-spin relaxation time measurements T_2 in porous zeolite control samples with known, uniformly distributed, moisture, was employed. Since T_2 values were found to be quite short, reaching $\sim$4 ms for low moisture contents, it was necessary to avoid the excessive spin-echo attenuation resulting from relatively long slice-selective radio-frequency (rf) pulses. To that end, we employed a three-dimensional (3D) gradient spin echo pulse sequence, where the short non- selective $\alpha = \pi/2$ rf pulse permits detection of spin echoes before severe T_2 attenuation takes place. Figure 3 shows schematically the sequence of rf and magnetic field gradient pulses employed. Here Gro denotes a readout gradient and Gpe 1 and Gpe 2 denote phase encoding gradients and T_E is spin-echo time.

Given that the longest spin-lattice relaxation time T_1 measured in the control samples was $\sim$25 ms, a recycling time $T_R = 60$ ms was employed in our measurements to minimize corrections due to T_1. Using an acquisition matrix of $128 \times 32 \times 32$, $T_R = 60$ ms, $T_E = 1$ ms, and four averages, each 3D image took 4 min. Except for the initial steps of water ingress, where profiles change quite rapidly, this finite imaging time is not expected to seriously affect time resolution.

Figure 4 shows water content profiles calculated from average signal amplitudes within the ROI. Due to the artifact shown on the left side of the images of Fig. 2, water content could not be measured for distances less than 4 mm. By using NMR imaging, rather than 1D projections [6], and with a ROI limited to a relatively narrow central region, we are

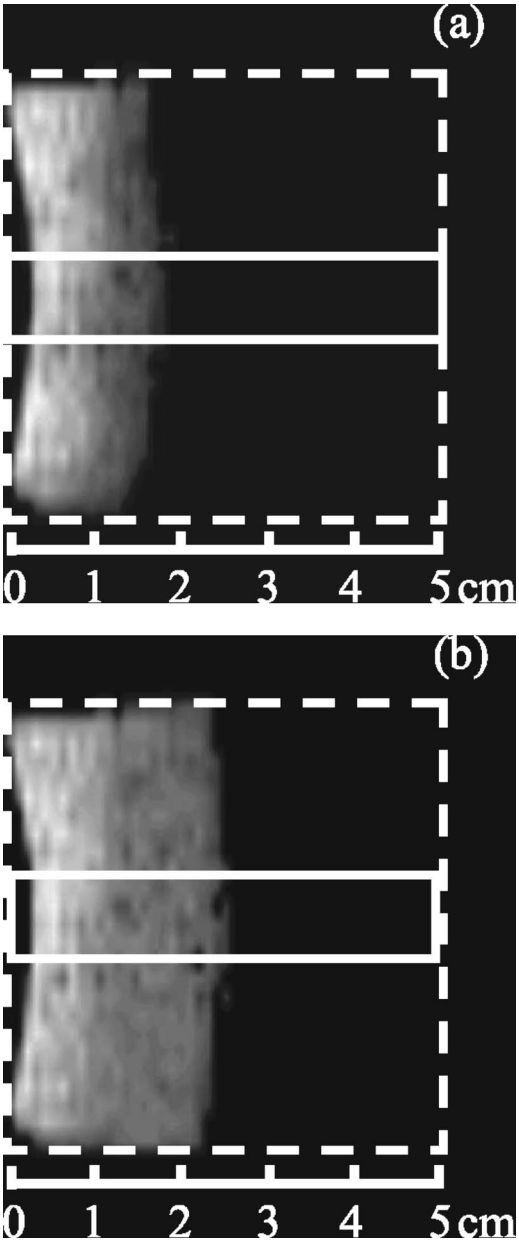

FIG. 2. Longitudinal NMR images of water ingress in a cylinder of compressed zeolite fine powder. Slices were selected through the center of the cylindrical sample. Time intervals after the beginning of water uptake are (a) 31 and (b) 182 min. Dashed rectangles show the sample boundary. White rectangles indicate the selected regions employed for moisture profile calculations.

able to obtain a good approximation of the boundary conditions required for Boltzmann's transformation.

IV. RESULTS AND DISCUSSION

Moisture transport in porous systems has been studied in great detail by several authors [19–21]. In order to define average quantities at a macroscopic level the system can be divided into representative volume elements which contain a sufficiently large number of pores to give statistical meaningful averages of quantities such as diffusivities. Average

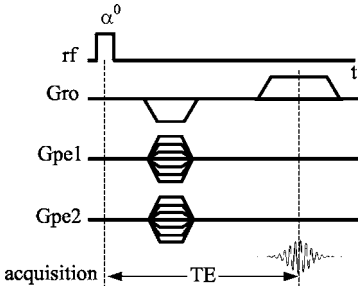

FIG. 3. Sequence of radio-frequency and magnetic field gradient pulses employed for imaging water ingress in a zeolite.

interparticle pore size in the solid matrix of porous zeolites is of order of several micrometers, but intraparticle pores of nanometric diameters are also present and are a distinctive feature of the zeolite structure.

For a description of moisture transport in unsaturated porous systems one needs to consider at least three components: liquid water, air-vapor mixture, and the solid matrix. The water component could further be considered to be in the form of liquid water or in the form of bound water adsorbed at the pore walls. However, since these two types of water molecules exchange very rapidly on an NMR time scale it is more appropriate to consider for the present purposes only a single water component, which on the average becomes less bound with increasing water concentration. This view is consistent with spin-spin relaxation rate measurements in control samples using a Carr-Purcell-Meiboom-Gill sequence [22] where single exponential decays were observed with relaxation rates exhibiting an approximately linear increase with inverse water concentration.

In a macroscopic description of moisture transport in porous systems several processes are known to contribute. Gra-

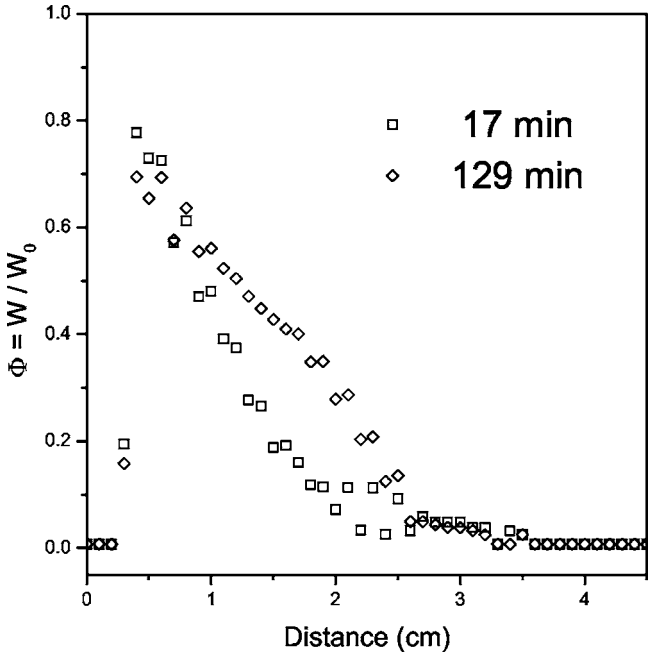

FIG. 4. Water content profiles along the axis of symmetry of the cylinder.

dients of capillary pressure lead to liquid transport while gradients of vapor pressure lead to vapor diffusion. Vapor pressure gradients can also cause liquid transport. If a water island is formed in a pore, with different vapor pressures on each side of the island, vapor will condense on one end and evaporate on the other end, leading to liquid transport. Another mechanism of water transport, which may act in parallel with the others, is surface diffusion by hopping along the pore wall.

All the above mechanisms of unsaturated moisture transport, combined with mass conservation, should lead to a diffusion equation Eq. (2), with an effective diffusivity $D_1(W)$ which is a function of only the local water concentration. Water ingress in a variety of porous solids such as fired-clay brick, sand-lime brick, and mortar has been shown to exhibit normal diffusive behavior [23,24] and obey Eq. (2). Also for some nonporous solids, like nylon 6.6, Eq. (2) was found to yield a correct description of water ingress [6]. For systems that obey Eq. (2), for the description of the water concentration dependence of the moisture diffusivity, an approximate exponential dependence of form $D_1(W)=D_1^{(0)}\exp(\alpha W/W_0)$ is usually adopted. Although significant departures from purely exponential behavior appear to prevail in some cases, values of the parameter α have been reported for various systems exhibiting normal diffusive behavior, such as $\alpha(\text{clay})=7.0$, $\alpha(\text{mortar})=8.0$, $\alpha(\text{sand-lime})=8.5$, and $\alpha(\text{nylon})=1.4$.

Water transport in porous systems consisting of fine zeolite powder compacted into a solid cylindrical rod appears to differ considerably from the cases mentioned above. Figure 5(a) shows moisture profiles, such as those of Fig. 4, plotted as a function of $\eta=x/t^{\gamma/2}$ ($\gamma=0.36$) for times ranging between 15 and 130 min. Unlike normal diffusion a collapse of all profiles appears to take place for $\gamma=0.36\pm0.04$ and not, as shown by Fig. 5(b), for $\gamma=1$. Moreover, water ingress into this system seems to have a considerable effect upon the porous structure. Thus, after water uptake to reach saturation, water removal by heating may lead to a different value of γ, which depends upon the heat treatment history.

The fractional-time diffusion equation model of subdiffusion is especially attractive because it should permit one to determine, from the double integral of Eq. (13), the functional dependence of $D_\gamma(W)$ for different values of γ and also compare with systems which exhibit normal diffusivity. As a consistency check we first tried in Eq. (13) the function $\Phi(\zeta)$ [Eq. (10)] corresponding to a constant D_γ solution. After performing the integrals the result yielded, as expected, a value of D_γ that was independent of local water concentration.

Since functions $\Phi(\zeta)$ with constant D_γ, given by Eq. (10), were not able to fit the data of Fig. 5(a) it was concluded that a concentration-dependent $D_\gamma(W)$ was needed. In order to determine $D_\gamma(W)$ from the data, using the double integral of Eq. (13), we chose to employ a fitting function to represent the experimental decay $\Phi(\eta)=W/W_0$ of Fig. 5(a). To that end we adopted a two-parameter function consisting of a product of the constant D_1 solution $1-\text{erf}(\eta/a)$ and an apodizing function of form $[1+(\eta/b)^n]^{-1}$, where a, b, and n are adjustable parameters. The result for $a=b=0.574\ \text{cm/s}^{0.18}$ and $n=4$ is shown as a solid line in Fig. 5(a). Once an analytical form of a fitting function has been determined, within the experimental uncertainty, one can use it to evaluate the double integral in Eq. (13) as well as to estimate the error in the calculated values of D_γ.

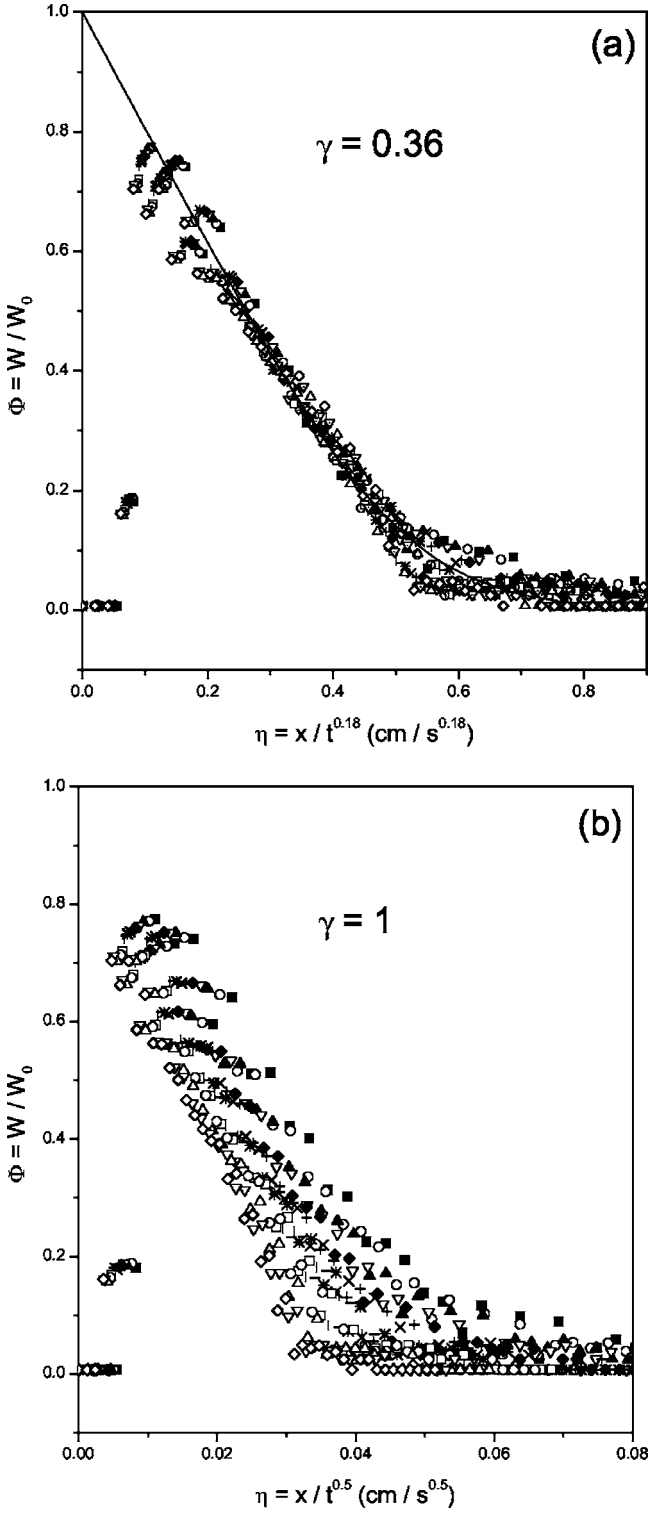

FIG. 5. Moisture profiles for various times in the range $15\leqslant t\leqslant 130$ min plotted as a function of $\eta=x/t^{0.18}$. The solid line represents the two-parameter fitting function employed in the calculation of $D_\gamma(W)$. (b) Same data plotted as a function of $\eta=x/t^{0.5}$ ($\gamma=1$).

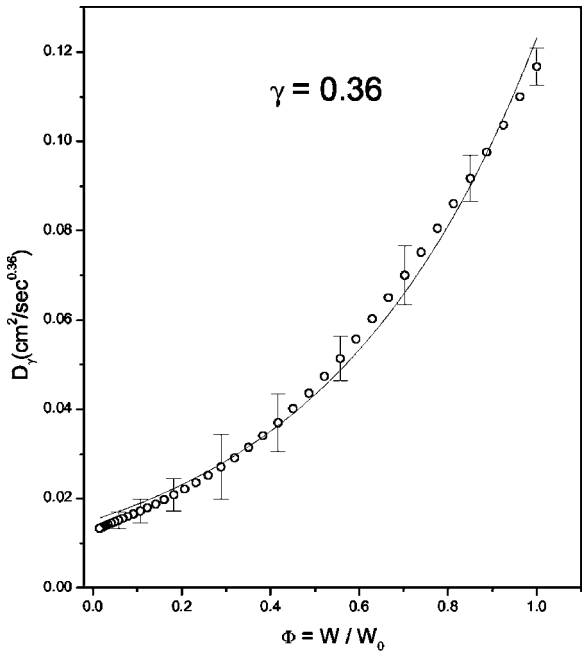

FIG. 6. Symbols, calculated values of $D_\gamma(W)$. Solid line is an exponential fit to the moisture dependence of the generalized diffusivity.

Figure 6 shows values of $D_\gamma(W)$ obtained from Eq. (13) and the fitting function that best adjusts the data of Fig. 5. The error bars were estimated by varying the parameters a and b in order to determine upper and lower bounds that take into account the dispersion of the data in Fig. 5. Figure 6 also shows an exponential function $D_\gamma(W)=D_\gamma^{(0)}\exp(\alpha W/W_0)$ with $D_\gamma^{(0)}=0.0152$ cm^2/s$^{0.36}$ and $\alpha=2.1$, which, in spite of some departures, appears to represent reasonably well the calculated moisture dependence of the generalized diffusivity $D_\gamma(W)$.

From the point of view of water transport an important aspect of zeolites, as opposed, for example, to fired-clay brick, mortar, and other similar porous systems, displaying normal diffusive behavior, may be related to very slowly decaying structural changes caused by water uptake. This has been recognized as a precondition for non-Fickian behavior [7]. Irreversible changes in the pore structure that occur as water ingresses into a fine particle zeolite powder compacted by high pressure may be responsible for the anomalous behavior shown in Fig. 5.

From the point of view of fractal time Brownian motion anomalous diffusion originates in a random walk with random waiting times T_i between successive jumps. The probability distribution [25] of waiting times is characterized by a long tail $P(T_i>t)=At^{-\gamma}$ $(0<\gamma<1)$ with a mean value $\langle T_i\rangle=\infty$. The time-fractional diffusion equation model of anomalous diffusion not only incorporates these concepts but should also permit one to draw additional conclusions concerning the moisture dependence of the effective diffusivity. Our results indicate that the measured value $\gamma=0.36$ is not a universal characteristic of zeolite systems but that it rather depends upon their previous history. As an example, two other samples subjected to different thermal treatment exhibited values $\gamma=0.64$ and 0.84, respectively. Strikingly, only relatively small changes in the moisture dependence of the effective diffusivity $D_\gamma(W)$, obtained from Eq. (13), were found in all three cases in spite of the large changes in the dynamics. As the values of γ approach unity the departures from a purely exponential behavior become somewhat more pronounced than in Fig. 6. However, the total variation of the monotonically increasing functions, represented by the ratio $D_\gamma(W\approx W_0)/D_\gamma(W\approx 0)$, was found to be almost independent of γ. Thus if one defines the parameter α more generally as $\alpha=\ln[D_\gamma(W\approx W_0)/D_\gamma(W\approx 0)]$, the results vary little with γ changing only from $\alpha=2.1$ to 2.4.

We conclude that the fractional-time diffusion equation approach is not only capable of predicting the scaling with $\eta=x/t^{\gamma/2}$ $(0<\gamma<1)$ of Boltzmann's test in a system exhibiting subdiffusion. It also permits determination of the moisture dependence of the generalized diffusivity. Although vastly different dynamics were apparent for zeolite samples with different values of γ the moisture dependence of the generalized diffusivity was little affected. This supports the view that the fractional-time diffusion approach actually addresses underlying physical processes, such as the moisture dependences of the capillary pressure, the vapor diffusion, and the pore diffusion, which appear to prevail, with little change, in normal as well as in anomalous transport. Moreover, the growth parameter α defined as $\alpha=\ln[D_\gamma(W\approx W_0)/D_\gamma(W\approx 0)]$ $(0<\gamma<1)$, appears to be a relatively robust characteristic of the system independently of the value of γ.

ACKNOWLEDGMENTS

This work has been supported by Conselho Nacional de Desenvolvimento Científico e Tecnológico and by PETROBRAS.

[1] H. Sher and E. Montroll, Phys. Rev. B **12**, 2455 (1975).
[2] Q. Gu, E. A. Schiff, S. Grebner, and R. Schwarz, Phys. Rev. Lett. **76**, 3196 (1996).
[3] F. Ambland, A. C. Maggs, B. Yurke, A. N. Pargellis, and S. Leibler, Phys. Rev. Lett. **77**, 4470 (1996).
[4] A. Klemm, R. Metzler, and R. Kimmich, Phys. Rev. E **65**, 021112 (2002).
[5] J. P. Bouchand and A. Georges, Phys. Rep. **195**, 127 (1990).
[6] S. Blackband and P. Mansfield, J. Phys. C **19**, L49 (1986).
[7] J. Crank, *The Mathematics of Diffusion* (Oxford University Press, London, 1975).
[8] P. D. M. Hughes, P. J. McDonald, M. R. Halse, B. Leone, and E. G. Smith, Phys. Rev. B **51**, 11332 (1995).
[9] P. D. M. Hughes, P. J. McDonald, and E. G. Smith, J. Magn.

Reson., Ser. A **121**, 147 (1996).
[10] K. S. Miller and B. Ross, *An Introduction to the Fractional Calculus and Fractional Differential Equations* (John Wiley, New York, 1993).
[11] Ralf Metzler, Eli Barkai, and Joseph Klafter, Phys. Rev. Lett. **82**, 3563 (1999).
[12] R. Metzler and J. Klafter, Phys. Rep. **339**, 1 (2000).
[13] E. Barkai, R. Metzler, and J. Klafter, Phys. Rev. E **61**, 132 (2000).
[14] R. Metzler and T. F. Nonnenmacher, Chem. Phys. **284**, 67 (2002).
[15] R. Hilfer, J. Phys. Chem. B **104**, 3914 (2000).
[16] W. L. Vargas, L. E. Palacio, and D. M. Dominguez, Phys. Rev. E **67**, 026314 (2003).
[17] E. K. Lenzi, R. S. Mendes, and C. Tsallis, Phys. Rev. E **67**, 031104 (2003).
[18] P. A. Webb and C. Orr, *Analytical Methods in Fine Particle Technology*, (Micromeritics Instrument Corporation, Norcross, 1997), p. 130.
[19] J. Bear and Y. Bachmat, *Introduction to Modeling of Transport Phenomena in Porous Media* (Kluwer, Dordrecht, The Nederlands, 1987), Vol. 4.
[20] J. R. Philip and D. A. de Vries, Trans., Am. Geophys. Union **38**, 222 (1957).
[21] Peischi Chen and D. C. T. Pei, Int. J. Heat Mass Transfer **32**, 297 (1989).
[22] S. Meiboom and D. Gill, Rev. Sci. Instrum. **29**, 688 (1958).
[23] L. Pel, H. Brocken, and K. Kopinga, Int. J. Heat Mass Transfer **39**, 1273 (1996).
[24] Relatively small departures from purely diffusive behavior and some evidence of anomalous transport have been more recently reported in these materials. Michel Kuntz and Paul Lavalée, J. Phys. D **34**, 2547 (2001).
[25] Karina Weron and Marcin Kotulski, Physica A **232**, 180 (1996).